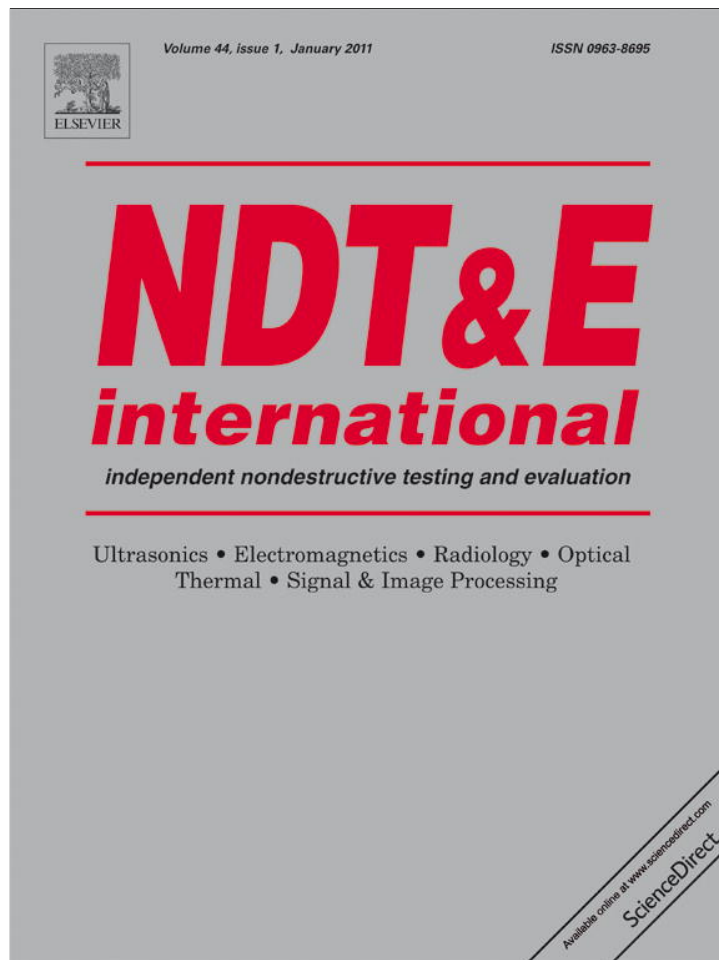


Provided for non-commercial research and education use.
Not for reproduction, distribution or commercial use.



This article appeared in a journal published by Elsevier. The attached copy is furnished to the author for internal non-commercial research and education use, including for instruction at the authors institution and sharing with colleagues.

Other uses, including reproduction and distribution, or selling or licensing copies, or posting to personal, institutional or third party websites are prohibited.

In most cases authors are permitted to post their version of the article (e.g. in Word or Tex form) to their personal website or institutional repository. Authors requiring further information regarding Elsevier's archiving and manuscript policies are encouraged to visit:

<http://www.elsevier.com/copyright>



Contents lists available at ScienceDirect

NDT&E International

journal homepage: www.elsevier.com/locate/ndteint

Calculation of propagation properties of Lamb waves in a functionally graded material (FGM) plate by power series technique

Xiaoshan Cao^a, Feng Jin^b, Insu Jeon^{a,*}

^a School of Mechanical Systems Engineering, Chonnam National University, 300 Yongbong-dong, Buk-gu, Gwangju 500-757, Republic of Korea

^b MOE Key Laboratory for Strength and Vibration, School of Aerospace, Xi'an Jiaotong University, Xi'an 710049, PR China

ARTICLE INFO

Article history:

Received 15 June 2009

Received in revised form

20 September 2010

Accepted 21 September 2010

Available online 29 September 2010

Keywords:

Functionally graded material (FGM)

Lamb waves

Dispersion relations

Wave structure

Ellipticity of particle trajectories

Ultrasonic nondestructive evaluation

ABSTRACT

To investigate the propagation behavior of Lamb waves in a thermal stress relaxation type functionally graded material (FGM) plate with material parameters that vary continuously along the thickness, the power series technique, which has been proved to have good convergence and high precision, is employed for theoretical derivations. The influence of the gradient coefficients of FGM on the dispersion curves is illustrated. The numerical results also reveal differences between the properties of Lamb wave propagation in the FGM plate and the corresponding properties in a homogenous plate. In terms of results, we find that both the normal and anomalous dispersions exist in the first and the second modes of the Lamb wave that propagates in the FGM plate, while only the anomalous dispersion is in the first mode and only the normal dispersion is in the second mode for the homogenous plate. The wave structure is asymmetric due to the asymmetric properties of the material. The dominance of in-plane and out-plane displacements is different between the metal-rich and ceramic-rich surfaces. All these results give theoretical guidance not only for experimental measurement of material properties but also for nondestructive evaluation using an ultrasonic wave generation device.

© 2010 Elsevier Ltd. All rights reserved.

1. Introduction

Functionally graded material (FGM) is a special kind of composite material wherein the volume fractions of two or more materials vary continuously. It is widely used in engineering fields, such as aerospace engineering, automobile industry, and mechanical metallurgy [1]. For example, the most popular application of FGM in aerospace engineering is the thermal stress relaxation type, wherein the thermal barrier structure for high-temperature applications may form from a mixture of a kind of metal and ceramic and the composition is varied from a metal-rich surface to a ceramic-rich surface.

In addition, there exist many different kinds of FGM in other fields, such as welding materials, thick coatings, materials with machined surfaces, degradable biomaterials, and so on [2]. The evaluation of the mechanical properties of FGMs has been considered an important research topic for investigating the mechanical characteristics of FGM structures. However, the properties of FGM are often difficult to obtain because they are not constants but vary along the thickness of FGM. Normally, the technique of guide waves is used for nondestructively evaluating material properties as well as for investigating defects in

homogenous media [3]. This technique has also been used as a method for measuring the material properties of FGM, which include the elastic modulus, density, and so on.

To study the wave propagation behavior in an inhomogeneous medium, where the mechanical properties vary continuously along the thickness, analytical solutions have been obtained only for some special cases due to the complexity of the governing equations, especially for the plane strain waves, which include two coupling variables. Most of these early studies were focused on numerical methods. Liu et al. [4] studied surface waves in FGM plates by the application of the strip element method. Liu et al. [5] and Han et al. [6] investigated stress waves in FGM structures using linearly inhomogeneous elements and quadratic layer elements, respectively. A hybrid numerical method was introduced by Han and Liu [7] for analyzing the characteristics of waves and transient responses in FGM cylinders. The numerical studies have been carried out based on the method of dividing the plane layer into a large number of thin sub-layers and treating each of them as a homogenous layer. However, the problem with this approach is that the material properties of the medium are assumed to change discontinuously from one sub-layer to another sub-layer. The same assumption has been adopted in the research done by the traditional Thomson–Haskell matrix method [3].

Some reports on the asymptotic analysis of wave propagation in inhomogeneous media can also be found, such as the WKB (Wentzel–Kramers–Brillouin) method [8,9], special functions

* Corresponding author. Tel.: +82 62 530 1688; fax: +82 62 530 1689.
E-mail address: i_jeon@chonnam.ac.kr (I. Jeon).

[10], the perturbation technique [11], and so on. The WKB method is always used to solve for the horizontal shear modes with only one component of displacement. Cao et al. [12] discussed the dispersion relations of Rayleigh wave in an FGM (functionally graded piezoelectric material) half-space, wherein the phase velocity is limited to a small scale. Through cylindrical functions, Vlasie and Rousseau [10] discussed Lamb wave propagation at high frequency in an FGM plate; they assumed a constant density and selected particular functions for the elastic parameters. Even though the variation in material parameters was limited in this special case, some parts of the dispersion curves could not be described due to the convergence condition of the method. Liu and Wang [11] studied the dispersion relations of Rayleigh waves in an FGM half-space by using the perturbation technique. However, all the analytical methods have their limitations: the WKB method can be used only at high frequencies, the special functions are suitable only for the special cases, and the perturbation technique is suitable for small gradient coefficients.

In the present study, we focus on the calculation of propagation properties of Lamb waves in a functionally graded material (FGM) plate using power series technique. As discussed above, some numerical [4–7] and analytical methods [8–11] have been carried out to study the wave propagation behavior in an inhomogeneous medium with material properties varying continuously along the depth direction. Compared with these methods, the power series technique developed in this study has many merits in describing the wave propagation behavior in FGM because the high precision solution and good convergence can be easily obtained through iterative calculation process.

Using the power series technique, the influence of the gradient functions and the gradient coefficients on dispersion relations of Lamb waves in this structure is quantified. The dispersion properties will change because of the inhomogeneous material. Due to the asymmetric properties of the FGM plate, the mode of particles' motion does not show symmetric characteristics as that in an isotropic plate. The asymmetric wave structures are shown in this paper. Furthermore, in order to describe the relative dominance between in-plane and out-plane displacements, the relationship between ellipticity of particle trajectories at the free surface and the wave number is discussed.

2. Statement of the problem

The propagation behavior of Lamb waves in an FGM plate, with a thickness of h , as shown in Fig. 1, will be taken into account. It is assumed that the mechanical properties of the FGM vary continuously along the thickness (the z -axis), i.e., all the properties, such as Lamé's constants, λ and μ , and mass density ρ , are functions of the z -axis. We consider the problem of plane deformations, wherein the motion is restricted in the xoz plane and the Lamb waves propagate in the positive direction of the x -axis.

Owing to the assumption of plane strain, the displacement components can be described as

$$u = u(x, z, t), \quad v = 0, \quad w = w(x, z, t) \quad (1)$$



Fig. 1. FGM plate structure and Cartesian coordinates.

The motion equation possesses the following form:

$$\frac{\partial \sigma_x}{\partial x} + \frac{\partial \tau_{xz}}{\partial z} = \rho \ddot{u}, \quad \frac{\partial \tau_{xz}}{\partial x} + \frac{\partial \sigma_z}{\partial z} = \rho \ddot{w} \quad (2)$$

where σ_x , σ_z , and τ_{xz} are the stress components, ρ is the mass density of the medium, and the dot “•” represents differentiation with respect to time. The relationships between displacement and strain components are

$$\varepsilon_x = \frac{\partial u}{\partial x}, \quad \varepsilon_z = \frac{\partial w}{\partial z}, \quad \gamma_{xz} = \frac{\partial u}{\partial z} + \frac{\partial w}{\partial x} \quad (3)$$

The constitutive equations of the functionally graded media can be expressed as follows:

$$\sigma_x = (\lambda + 2\mu)\varepsilon_x + \lambda\varepsilon_z, \quad \sigma_z = \lambda\varepsilon_x + (\lambda + 2\mu)\varepsilon_z, \quad \tau_{xz} = \mu\gamma_{xz} \quad (4)$$

where λ and μ are Lamé's constants. Substituting Eqs. (1), (3), and (4) into Eq. (2), we obtain the following field equations for the FGM plate:

$$(\lambda + 2\mu) \frac{\partial^2 u}{\partial x^2} + \lambda \frac{\partial^2 w}{\partial x \partial z} + \mu \left(\frac{\partial^2 w}{\partial x \partial z} + \frac{\partial^2 u}{\partial z^2} \right) + \mu' \left(\frac{\partial w}{\partial x} + \frac{\partial u}{\partial z} \right) = \rho \ddot{u} \quad (5)$$

$$(\lambda + 2\mu) \frac{\partial^2 w}{\partial z^2} + \lambda \frac{\partial^2 u}{\partial x \partial z} + \mu \left(\frac{\partial^2 w}{\partial x^2} + \frac{\partial^2 u}{\partial x \partial z} \right) + \lambda' \frac{\partial u}{\partial x} + (\lambda + 2\mu)' \frac{\partial w}{\partial z} = \rho \ddot{w} \quad (6)$$

where the superscript “ ’ ” indicates space differentiation with respect to the z -coordinate.

For Lamb waves that propagate in the FGM plate, the traction free boundary condition should be satisfied at the top and bottom surfaces, that is

$$\sigma_z(x, 0) = 0, \quad \tau_{xz}(x, 0) = 0, \quad \sigma_z(x, h) = 0, \quad \tau_{xz}(x, h) = 0 \quad (7)$$

3. Solution of the problem

For the Lamb waves in the inhomogeneous plate described above, the solution of the governing equations can be expressed in the following form:

$$u(x, z, t) = Z_u(z) \exp(ikx - ikct) = Z_u(z) \exp(ikx - i\omega t) \quad (8)$$

$$w(x, z, t) = Z_w(z) \exp(ikx - ikct) = Z_w(z) \exp(ikx - i\omega t) \quad (9)$$

where $i = \sqrt{-1}$, $k = 2\pi/\lambda$ is the wave number with λ being the wavelength, c the phase velocity, and $Z_u(z)$ and $Z_w(z)$ are the unknown amplitudes of the displacement components. Substituting Eqs. (8) and (9) into Eqs. (5) and (6), we obtain

$$\mu Z_u'' + \mu' Z_u' + (\lambda + \mu) ik Z_w' + (\rho c^2 - \lambda - 2\mu) k^2 Z_u + \mu' ik Z_w = 0 \quad (10)$$

$$(\lambda + 2\mu) Z_w'' + (\lambda + \mu) ik Z_u' + (\lambda + 2\mu)' Z_w' + \lambda' ik Z_u + (\rho c^2 - \mu) k^2 Z_w = 0 \quad (11)$$

It is assumed that the parameters of the FGM possess the following form:

$$\lambda = f_1 \left(\frac{z}{h} \right), \quad \mu = f_2 \left(\frac{z}{h} \right), \quad \rho = f_3 \left(\frac{z}{h} \right) \quad (12)$$

Because of the fact that the parameters of the FGM are continuously variable, they can be expressed by the power series as

$$f_i \left(\frac{z}{h} \right) = \sum_{n=0}^{\infty} a_n^i \left(\frac{z}{h} \right)^n \quad (13)$$

where $i = 1-3$.

It is assumed that $\tilde{Z}_u = Z_u$ and $\tilde{Z}_w = iZ_w$; then Eqs. (10) and (11) can be transformed into the following forms:

$$\mu \tilde{Z}_u'' + \mu' \tilde{Z}_u' + (\lambda + \mu)k \tilde{Z}_w' + (\rho c^2 - \lambda - 2\mu)k^2 \tilde{Z}_u + \mu' k \tilde{Z}_w = 0 \quad (14)$$

$$(\lambda + 2\mu)\tilde{Z}_w'' - (\lambda + \mu)k \tilde{Z}_u' + (\lambda + 2\mu)\tilde{Z}_w' - \lambda' k \tilde{Z}_u + (\rho c^2 - \mu)k^2 \tilde{Z}_w = 0 \quad (15)$$

The solutions of Eqs. (14) and (15) can take the following forms:

$$\tilde{Z}_u = \sum_{n=0}^{\infty} s_n \left(\frac{z}{h}\right)^n, \quad \tilde{Z}_w = \sum_{n=0}^{\infty} t_n \left(\frac{z}{h}\right)^n \quad (16)$$

Substituting Eqs. (12), (13), and (16) into Eqs. (14) and (15), we obtain

$$\begin{aligned} & \left[\sum_{n=0}^{\infty} a_n^2 \left(\frac{z}{h}\right)^n \right] \left[\sum_{n=0}^{\infty} s_{n+2}(n+2)(n+1) \left(\frac{z}{h}\right)^n \right] \\ & + \left[\sum_{n=0}^{\infty} a_{n+1}^2 (n+1) \left(\frac{z}{h}\right)^n \right] \left[\sum_{n=0}^{\infty} s_{n+1}(n+1) \left(\frac{z}{h}\right)^n \right] \\ & + (kh)^2 \left[\sum_{n=0}^{\infty} (a_n^3 c^2 - a_n^1 - 2a_n^2) \left(\frac{z}{h}\right)^n \right] \left[\sum_{n=0}^{\infty} s_n \left(\frac{z}{h}\right)^n \right] \\ & + kh \left[\sum_{n=0}^{\infty} (a_n^1 + a_n^2) \left(\frac{z}{h}\right)^n \right] \left[\sum_{n=0}^{\infty} t_{n+1}(n+1) \left(\frac{z}{h}\right)^n \right] \\ & + kh \left[\sum_{n=0}^{\infty} a_{n+1}^2 (n+1) \left(\frac{z}{h}\right)^n \right] \left[\sum_{n=0}^{\infty} t_n \left(\frac{z}{h}\right)^n \right] = 0 \end{aligned} \quad (17)$$

$$\begin{aligned} & \left[\sum_{n=0}^{\infty} (a_n^1 + 2a_n^2) \left(\frac{z}{h}\right)^n \right] \left[\sum_{n=0}^{\infty} t_{n+2}(n+2)(n+1) \left(\frac{z}{h}\right)^n \right] \\ & + \left[\sum_{n=0}^{\infty} (a_{n+1}^1 + a_{n+1}^2)(n+1) \left(\frac{z}{h}\right)^n \right] \left[\sum_{n=0}^{\infty} t_{n+1}(n+1) \left(\frac{z}{h}\right)^n \right] \\ & + (kh)^2 \left[\sum_{n=0}^{\infty} (a_n^3 c^2 - a_n^2) \left(\frac{z}{h}\right)^n \right] \left[\sum_{n=0}^{\infty} t_n \left(\frac{z}{h}\right)^n \right] \\ & - (kh) \left\{ \left[\sum_{n=0}^{\infty} (a_n^1 + a_n^2) \left(\frac{z}{h}\right)^n \right] \left[\sum_{n=0}^{\infty} s_{n+1}(n+1) \left(\frac{z}{h}\right)^n \right] \right. \\ & \left. + \left[\sum_{n=0}^{\infty} a_{n+1}^2 (n+1) \left(\frac{z}{h}\right)^n \right] \left[\sum_{n=0}^{\infty} s_n \left(\frac{z}{h}\right)^n \right] \right\} = 0 \end{aligned} \quad (18)$$

By equating the coefficients of $(z/h)^n$ in Eqs. (17) and (18) to zero, we can obtain two recursive equations to determine s_n and t_n , as follows:

$$\begin{aligned} & \sum_{i=0}^n (i+2)(i+1)a_{n-i}^2 s_{i+2} + \sum_{i=0}^n (n-i+1)(i+1)a_{n-i+1}^2 s_{i+1} \\ & + (kh)^2 \sum_{i=0}^n (a_{n-i}^3 c^2 - a_{n-i}^1 - 2a_{n-i}^2) s_i + (kh) \sum_{i=0}^n (i+1)(a_{n-i}^1 + a_{n-i}^2) t_{i+1} \\ & + (kh) \sum_{i=0}^n (n-i+1)a_{n-i+1}^2 t_i = 0 \end{aligned} \quad (19)$$

$$\begin{aligned} & \sum_{i=0}^n (i+2)(i+1)(a_{n-i}^1 + 2a_{n-i}^2) t_{i+2} + \sum_{i=0}^n (n-i+1)(i+1)(a_{n-i+1}^1 + 2a_{n-i+1}^2) t_{i+1} \\ & + (kh)^2 \sum_{i=0}^n (a_{n-i}^3 c^2 - a_{n-i}^2) t_i - (kh) \left[\sum_{i=0}^n (i+1)(a_{n-i}^1 + a_{n-i}^2) s_{i+1} \right. \\ & \left. + \sum_{i=0}^n (n-i+1)a_{n-i+1}^2 s_i \right] = 0 \end{aligned} \quad (20)$$

where s_0, s_1, t_0 , and t_1 are undetermined coefficients and for $i \geq 2$ all of the s_i and t_i are linear functions of s_0, s_1, t_0 , and t_1 .

To determine the undetermined coefficients in the expressions of the solution, the following matrix is constructed:

$$(s_{0j}, s_{1j}, t_{0j}, t_{1j}) = I \quad (21)$$

where $j=1-4$ and I is a 4×4 unity matrix. Thus, the equivalent form of Eq. (16) is as follows:

$$\tilde{Z}_u = \sum_{j=1}^4 C_j \sum_{n=0}^{\infty} s_{nj} \left(\frac{z}{h}\right)^n, \quad \tilde{Z}_w = \sum_{j=1}^4 C_j \sum_{n=0}^{\infty} t_{nj} \left(\frac{z}{h}\right)^n \quad (22)$$

where C_j ($j=1-4$) are undetermined constants. For $n=0$ and 1, s_{nj} and t_{nj} satisfy expression (21), while for other values of n , s_{nj} and t_{nj} can be determined by Eqs. (19) and (20).

Substituting Eq. (22) into the boundary conditions, we can obtain linear algebraic equations with respect to C_i ($i=1-4$). From the sufficient and necessary condition that a non-trivial solution exists, the determinant of the coefficient matrix has to vanish, which leads to the following dispersion relation for Lamb waves:

$$|T_{ij}| = 0 \quad (23)$$

where

$$T_{11} = \lambda^0 kh, \quad T_{14} = -(\lambda^0 + 2\mu^0), \quad T_{22} = 1, \quad T_{23} = kh$$

$$T_{3j} = \sum_{n=0}^{\infty} [\lambda^h s_{nj} kh - (\lambda^h + 2\mu^h)(n+1)t_{(n+1)j}]$$

$$T_{4j} = \sum_{n=0}^{\infty} [t_{nj} kh + (n+1)s_{(n+1)j}], \quad j = 1-4$$

and all the other terms are equal to zero. Material parameters of the top and bottom surfaces of the FGM plate can be differentiated by the superscripts 0 and h .

For the thermal stress relaxation material with parameters that vary slowly, the asymptotic expansion of the displacement components can be obtained because of the convergence of the power series. For example, it is assumed that the parameters vary linearly, i.e., $a_n^i = 0$ for $i=1-3$ when $n \geq 2$. The following equations are deduced from the recurrence relations, Eqs. (19) and (20):

$$\lim_{n \rightarrow \infty} \frac{s_{n+1}}{s_n} = \frac{a_1^2}{a_0^2}, \quad \lim_{n \rightarrow \infty} \frac{t_{n+1}}{t_n} = \frac{a_1^2 + 2a_1^1}{a_0^2 + 2a_0^1}$$

where a_0 and a_1 with superscripts 1 and 2 are defined in Eq. (13).

Let us consider the coordinate plane in which Lamé's constants satisfy the inequalities, $|a_1^2/a_0^2| < 1$ and $|(a_1^2 + 2a_1^1)/(a_0^2 + 2a_0^1)| < 1$. According to the theorem of convergent criterion of power series, this solution is convergent. For other cases, convergence can be proved by mathematical induction.

4. Numerical results and discussion

In numerical analysis, FGM is a functionally graded composite of two kinds of material, materials I and II, with the volume fractions of the materials varying along the thickness. The parameters of the FGM media are described as

$$g(z) = g^{(1)} f^{(1)}(z/h) + g^{(2)} f^{(2)}(z/h) \quad (24)$$

where $f^{(1)}$ and $f^{(2)}$ are the volume fractions and $g^{(1)}$ and $g^{(2)}$ indicate the parameters of materials I and II, respectively. Metal Cr and ceramics are chosen as materials I and II, respectively. Their material parameters are

$$\begin{aligned} \text{Cr: } & \rho^{(1)} = 7190 \text{ kg/m}^3, \quad \lambda^{(1)} = 74.2 \text{ Gpa}, \quad \mu^{(1)} = 102.5 \text{ Gpa} \\ \text{Ceramics: } & \rho^{(2)} = 3900 \text{ kg/m}^3, \quad \lambda^{(2)} = 138 \text{ Gpa}, \quad \mu^{(2)} = 118.11 \text{ Gpa} \end{aligned}$$

In this paper, two types of volume fractions are discussed, which are the exponential and power functions, i.e.

$$A: f^{(1)}\left(\frac{z}{h}\right) = 1 - \left(\frac{z}{h}\right)^{p_p} \quad (25)$$

$$f^{(1)}\left(\frac{z}{h}\right) = 1 - \frac{1 - \exp(p_e z/h)}{1 - \exp(p_e)} \quad (26)$$

with $f^{(2)}(z/h) = 1 - f^{(1)}(z/h)$, where p_p , which is a non-negative integer, and p_e are the gradient coefficients. The surface at $z=0$ is metal-rich while that at $z=h$ is ceramic-rich.

4.1. Dispersion curves

Fig. 2 shows the dispersion curves, where the dimensionless wave number, kh , is used as the abscissa. The physical meaning of kh is the product of 2π and the ratio of the thickness to the wavelength. We select the FGM where the volume fraction varies linearly, that is, $p_e=0$ in Eq. (25) and $p_p=1$ in Eq. (26).

Since there are obvious differences in the material properties between Cr and ceramics, the dispersion curves of these two kinds of plate are significantly different. The dispersion curves of Lamb waves in an FGM plate are between those for the two corresponding homogeneous plates. For a certain mode, the plates in descending order of the phase velocity of the Lamb waves are ceramic, FGM, and metallic. With the wave number and the phase velocity in a certain range, the results show that the number of modes of the Lamb waves in the FGM plate is more than that in the ceramic plate and less than that in the metallic plate.

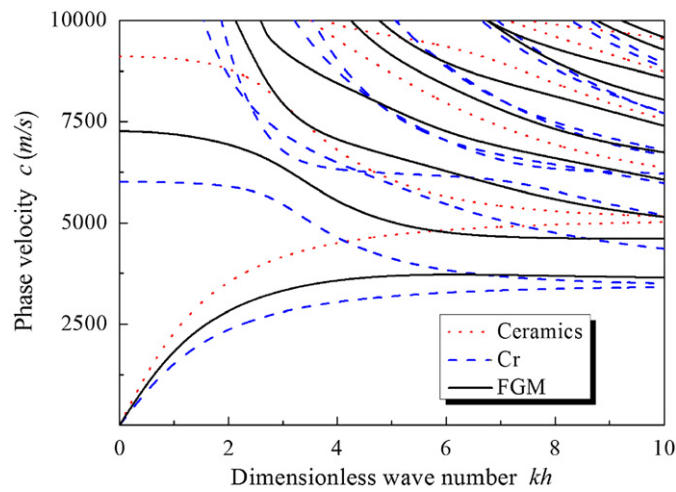


Fig. 2. Dispersion curves of Lamb waves in the plates of Cr, ceramic, and FGM.

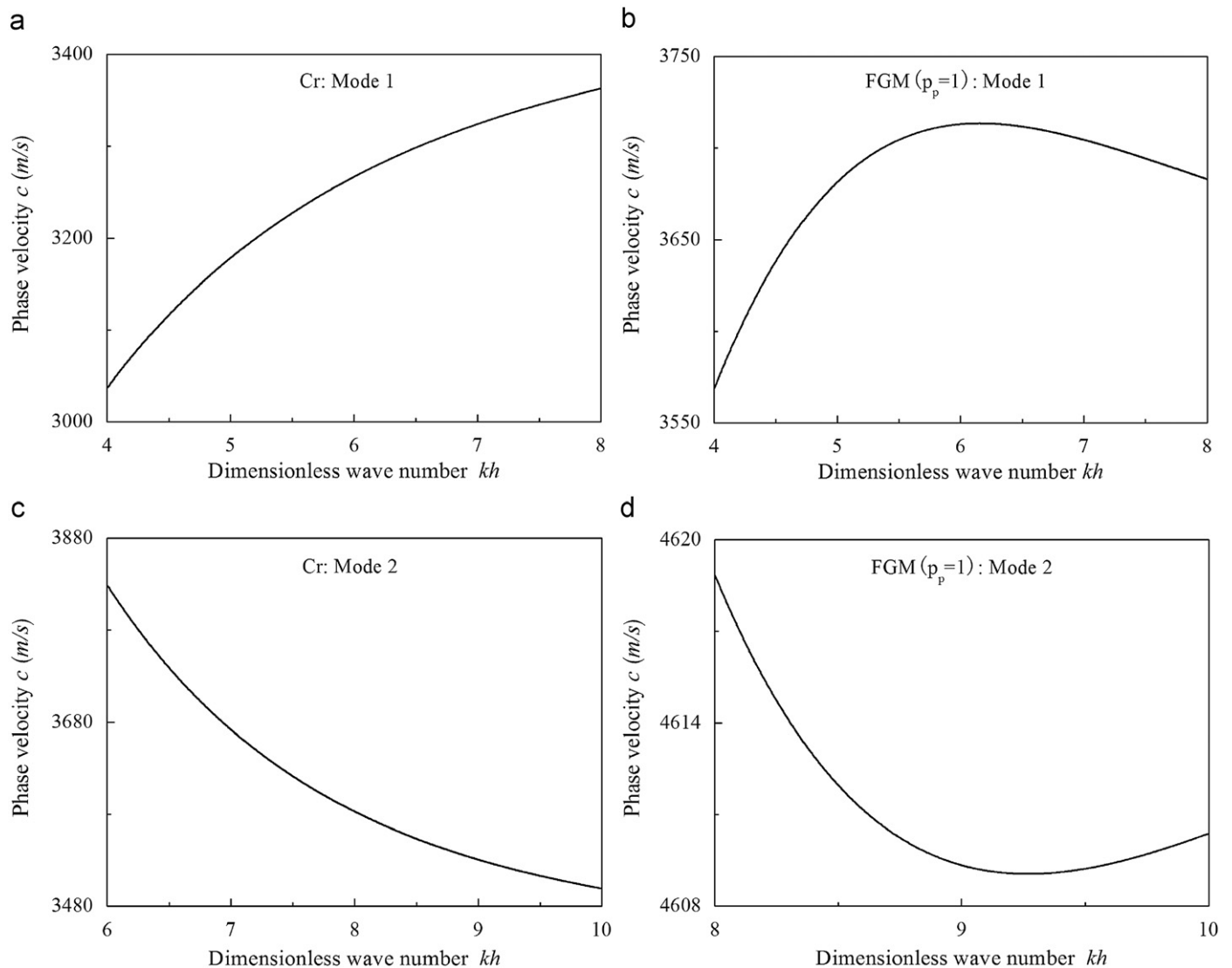


Fig. 3. Some details of dispersion curves of Lamb waves: (a) Cr (mode 1), (b) FGM ($p_p=1$, mode 1), (c) Cr (mode 2), and (d) FGM ($p_p=1$, mode 2).

For example, for the case when kh ranges from 0 to 10 and the phase velocity is less than 10000 m/s, as shown in Fig. 2, there exist six modes in the ceramic plate, 10 modes in the FGM plate, and 12 modes in the metallic plate.

Normally, the dispersion properties are determined by the relationship between the phase velocity and the group velocity. It is well known that the group velocity of wave propagation, which is defined as $c_g = c + kdc/dk$, expresses the rate at which energy is transported. If the group velocity is actually greater than the phase velocity (i.e., $dc/dk > 0$), the phenomenon is termed as anomalous dispersion; the converse (viz., $dc/dk < 0$) is named as normal dispersion. From Fig. 2, it is clear that both anomalous and normal dispersions occur in the Lamb waves in the homogenous and FGM plates. However, in the first mode, there is only anomalous dispersion in the homogenous plate, as shown in Fig. 2, with the details shown in Fig. 3(a), and only normal dispersion in the second mode, while the details are shown in Fig. 3(c). A comparison of the dispersion curves of the first mode in the FGM plate, as shown in the Fig. 3(b), where kh ranges from 4 to 8, reveals that the phase velocity reaches a maximum at $kh=6.2$. In the second mode, as revealed in Fig. 3(d), the phase velocity reaches a minimum at $kh=9.3$. In the dispersion curves, some parts satisfy $dc/dk > 0$ and the others satisfy $dc/dk < 0$ in the first and second modes. In other words, there are both anomalous and normal dispersions in the FGM plate. From the relationship between the phase velocity and the wave number, we can conclude that the dispersion properties of the first and second modes of the Lamb waves in the FGM plate are different from those in the homogenous plate.

The dispersion curves are influenced by not only the gradient functions but also the gradient coefficients, as shown in Fig. 4(a) and (b). Phase velocity and the number of modes are closely related to the gradient coefficient. For the two kinds of FGM plate, i.e., A and B, the phase velocity will decrease and the number of modes will increase with the increase in the gradient coefficient. In other words, the larger the gradient coefficient, the greater the percentage of metal in the FGM plate. Therefore, the dispersion curves of the Lamb wave in the FGM plate approach those of the metallic plate as the gradient coefficient increases. This conclusion can also be obtained from Fig. 5.

For the FGM plate, Lamb waves can be used for measuring the gradient coefficient. Fig. 5 shows the variation in the phase velocity for the first four modes, where c_m is the phase velocity of Lamb waves in the Cr plate. The point at $kh=2\pi$ indicates that the wavelength equals the thickness of the plate. For type A, p_p is a non-negative integer and discontinuous and for type B, p_e can be selected continually.

4.2. Wave structure analysis

Much research has been carried out on the variation in the wave structure as one increases the ωh product along a particular mode in the homogenous plate. Researchers are interested in the variation with the mode of the ratio of the in-plane to out-plane displacements. The use of a wave structure can lead to increased wave penetration power along the structure. Rose [3] has described the wave structures in a homogenous plate in detail. The displacement amplitude of Lamb waves in a homogenous plate is either symmetric or asymmetric. In the odd-numbered modes, the in-plane displacement is asymmetric and the out-plane displacement is symmetric but in the even-numbered modes, the situation is reversed.

However, because of the asymmetric properties of the FGM plate, the displacement amplitudes do not reveal a symmetric character as those in an isotropic plate. For example, when the wavelength equals

the thickness of the plate with the parameter varying linearly, the wave structures are shown in Fig. 6(a)–(d). For the first and third modes, the displacement amplitudes of the metal-rich surface are

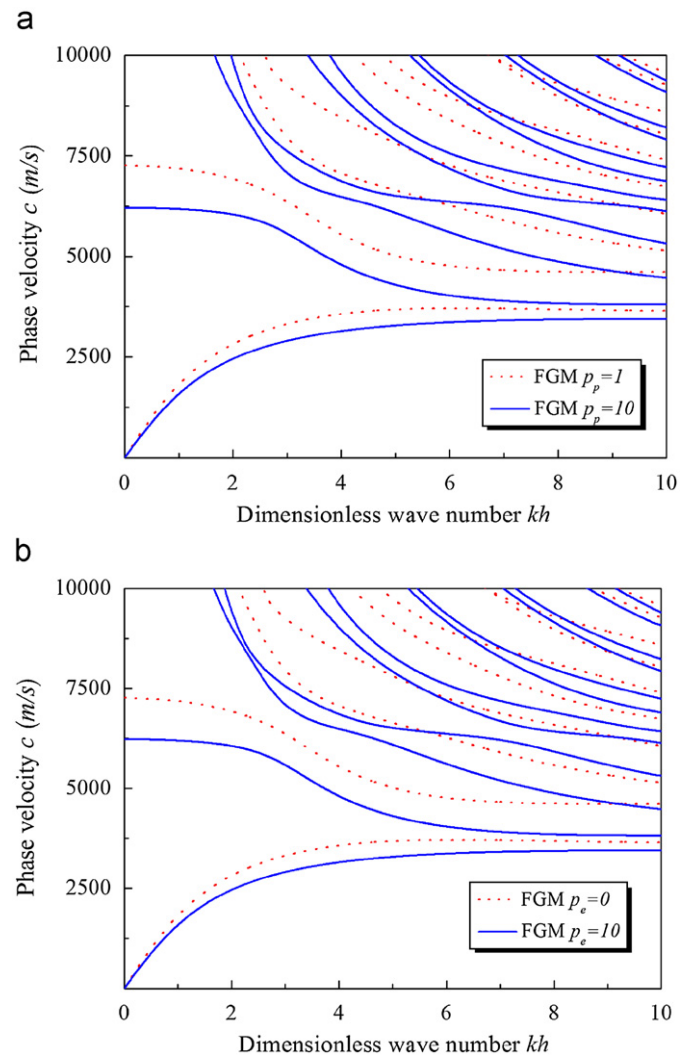


Fig. 4. Influence of gradient coefficient on dispersion curves: (a) A type and (b) B type.

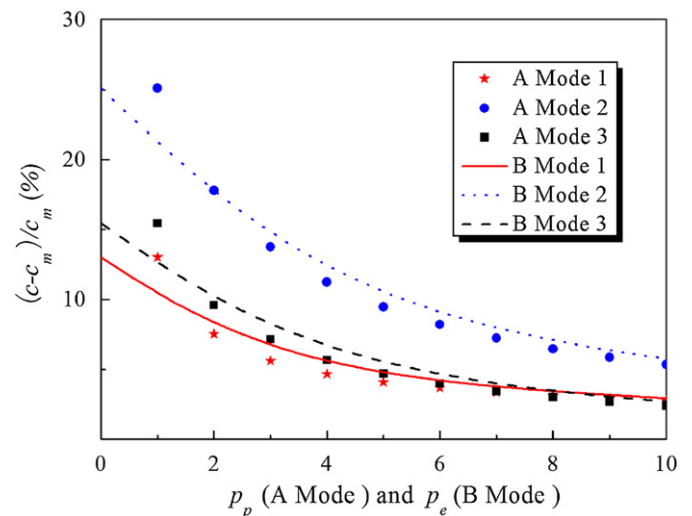


Fig. 5. Influence of gradient coefficient on phase velocity at $kh=2\pi$.

more obvious than those of the ceramic-rich surface but the situation is reversed in the second mode. There is an interesting result in the fourth mode, namely, that in the metal-rich surface, the dominant position is the in-plane displacement whereas it is the out-plane displacement in the ceramic-rich surface.

4.3. Ellipticity of particle trajectories at free surface

In research on Lamb waves that propagate in a homogenous plate, some attention has been focused on the point where the dominant displacement is either the out-plane displacement, w , or the in-plane displacement, u . Due to the symmetric properties, the ratios of the amplitude of out-plane displacement to that of in-plane displacement at the top and bottom surfaces are reciprocals. However, in the FGM plate, their absolute values should be different. The difference between the ratios for the top and bottom surfaces might imply that the dominant position of the metal-rich surface is not the same as that of the ceramic-rich surface.

When the Lamb wave propagates, the trajectories of the particles are ellipses. To discuss the relationships between the displacement components on the surface, we denote the ellipticity of particle

trajectories by $|\gamma_0| = |w_0|/|u_0|$ and $|\gamma_h| = |w_h|/|u_h|$, where $|w_0|$, $|u_0|$ and $|w_h|$, $|u_h|$ are the amplitudes of displacement components of the bottom and top surfaces, respectively. The sign of the ellipticity of particle trajectories is determined by the direction of the particle trajectories. When the trajectories are anticlockwise, the ellipticity of particle trajectories has a positive sign; otherwise, it is negative sign. According to the definition of ellipticity, when the absolute value is much larger than unity, the out-plane displacement is the dominant one. Otherwise, when the absolute value is much smaller than unity, the in-plane displacement is the dominant one.

Fig. 7(a)–(d) clarifies the difference between the metal-rich and ceramic-rich surfaces with regard to the ellipticity of particle trajectories. For the first mode, the absolute values of ellipticities are almost the same. For the second mode, when the dimensionless wave number is very small, the dominant displacement in both the metal-rich and ceramic-rich surfaces is the in-plane displacement, while all the absolute values of the ellipticity of particle trajectories are much smaller than unity. Initially, as the dimensionless wave number increases, the absolute value of the particle trajectories' ellipticity gradually increases, i.e., the out-plane displacement gradually becomes dominant. However, after the point where the ellipticity of the particle trajectories

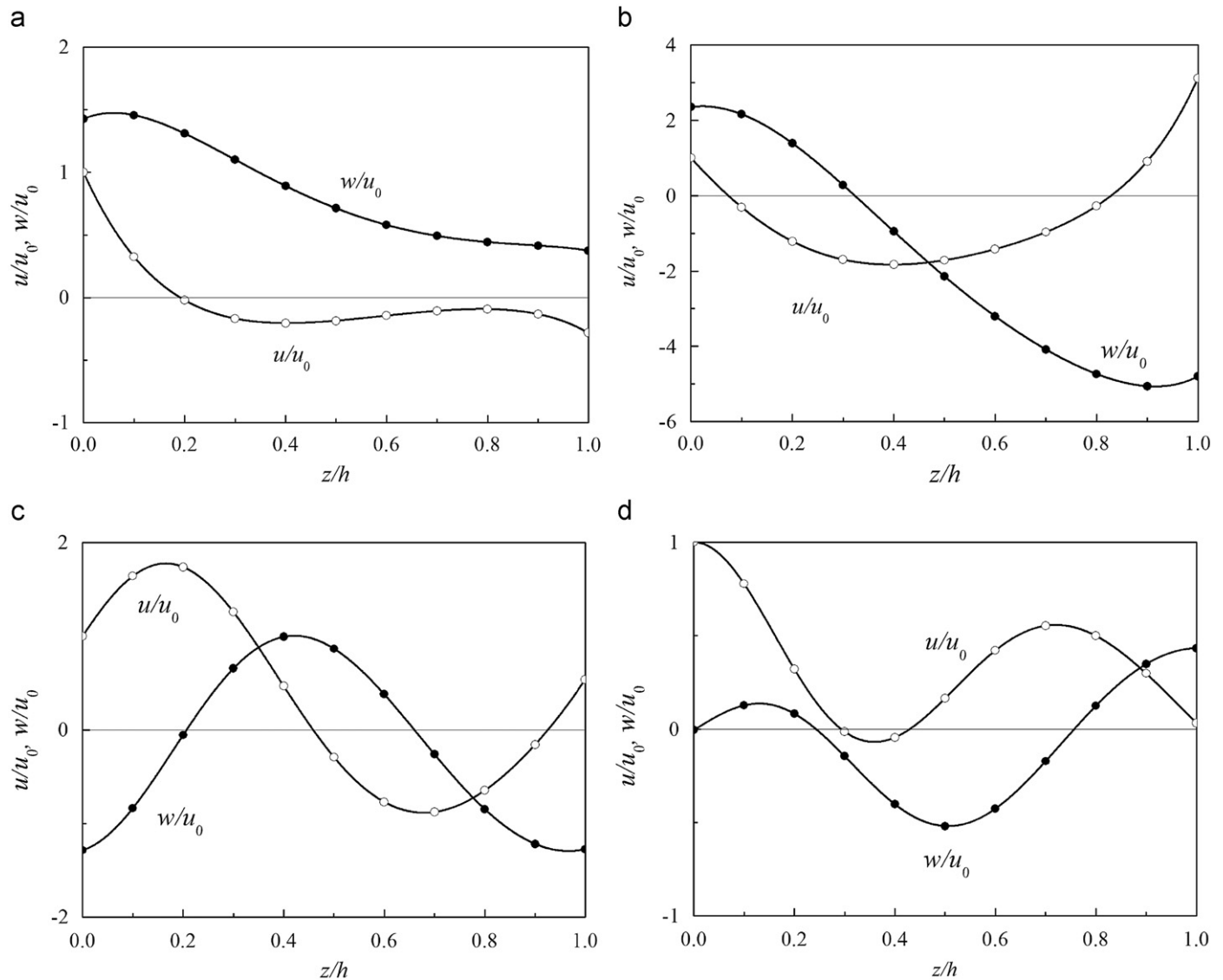


Fig. 6. Wave structure at $kh=2\pi$: (a) mode 1, (b) mode 2, (c) mode 3, and (d) mode 4.

asymptotically approaches infinity, namely, the in-plane displacement approaches zero, the absolute value of the particle trajectories' ellipticity gradually decreases. The variations in the upper and bottom surfaces are almost similar with a minor difference being that the changes in the ceramic-rich surface precede those in the metal-rich surface. For the third and fourth modes, the difference in the absolute value of the particle trajectories' ellipticity between the metal-rich and ceramic-rich surfaces is conspicuous. A point is observed where the dominant displacement is entirely different between the ceramic-rich and metal-rich surfaces. For example, for the fourth mode, when kh is about 6, the absolute value of the particle trajectories' ellipticity in the ceramic-rich surface is much larger than unity, while that in the metal-rich surface approaches zero. In other words, in the metal-rich surface, the in-plane displacement is dominant but the opposite is the case in the ceramic-rich surface. A similar situation also arises in the third mode, when kh is about 2.8.

4.4. Precision of the solution

On one hand, the dispersion relation, Eq. (23), is not only for Lamb waves in the FGM plate but also for the homogenous plate.

To illustrate convergence, we consider a relatively simple problem that has a known solution, which is the Lamb wave propagation in a homogenous plate. Fig. 8 presents the dispersion relations that are calculated through the present power series solution wherein the first 50 terms are retained. It can be seen clearly from Fig. 2 that for each mode of the Lamb wave phase velocities, the numerical results obtained with the first 50 terms in the series agree well with the analytical solutions. Consequently, in all the above numerical calculations, the following convergent criterion is adopted for phase velocity analysis:

$$\frac{|c|_{n=N} - c|_{n>N}|}{c|_{n=N}} < \varepsilon$$

where c_n is the solution of the phase velocity from the first n terms of the power series. In this paper, $\varepsilon=0.001\%$ is selected in all the numerical examples, while $c|_{n>N}$ is replaced by $c|_{n=2N}$.

On the other hand, few analytical solutions have been published on Lamb wave propagation in FGM plates. The popular method for this problem is to treat the FGM plate as a multi-layered structure where each layer is homogenous. In this paper, we discuss a comparison between the results from the global matrix method and the power series method. For example, we select an FGM for which

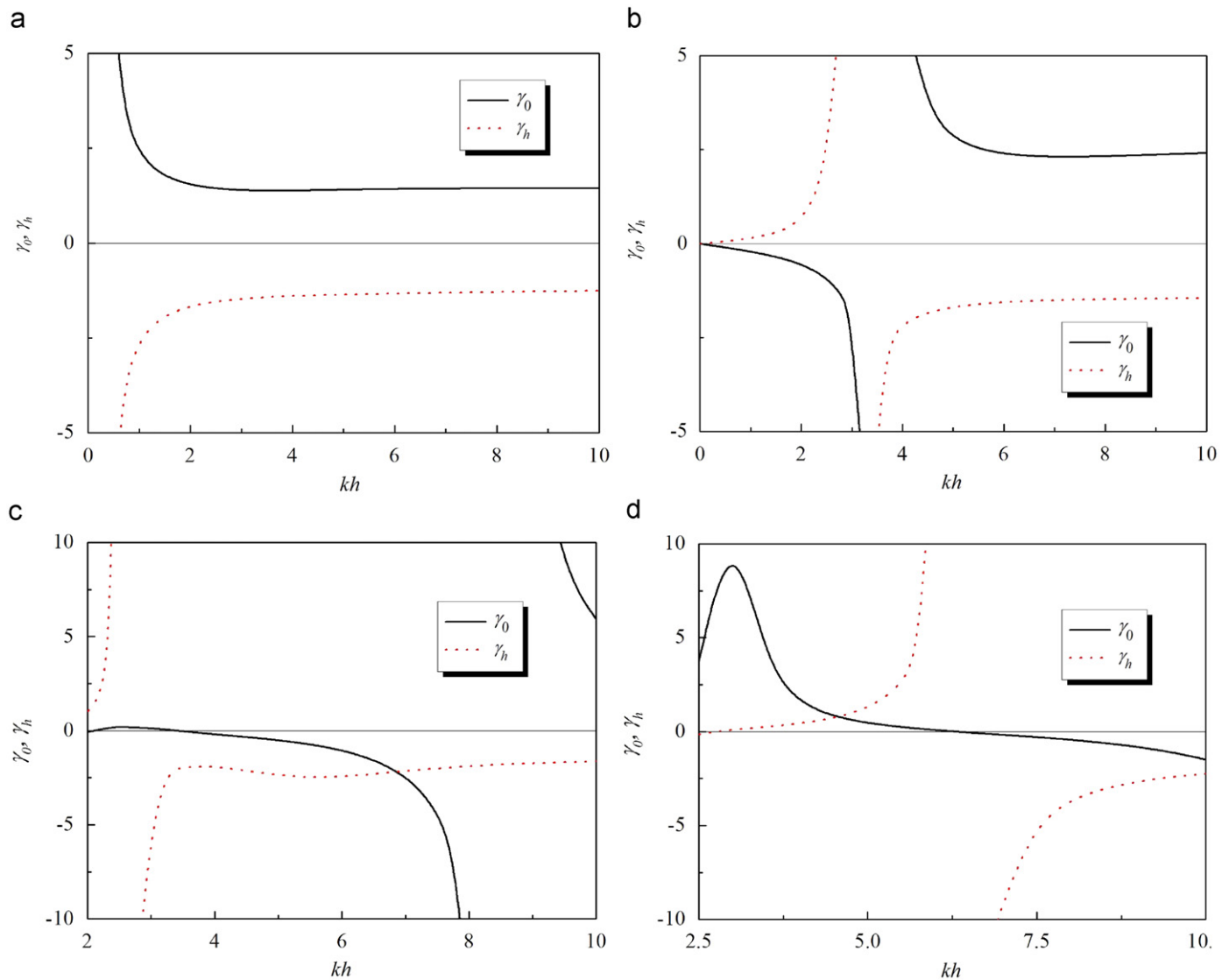


Fig. 7. Ellipticity of particle trajectories at the free surface: (a) mode 1, (b) mode 2, (c) mode 3, and (d) mode 4.

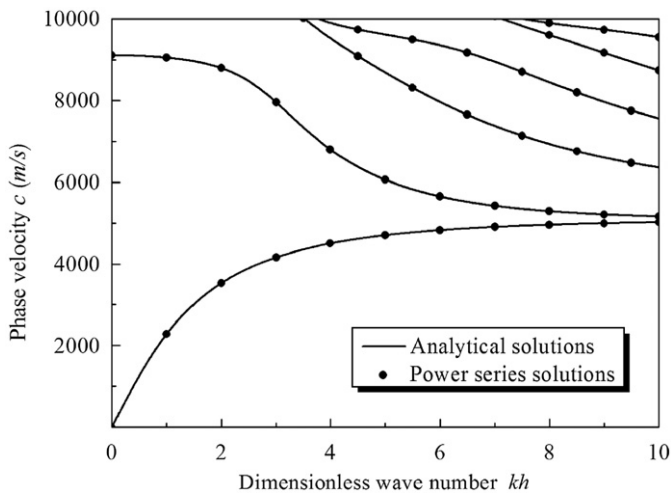


Fig. 8. Comparison of the dispersion curves in the ceramic plate obtained from the analytical solution and the power series solution.

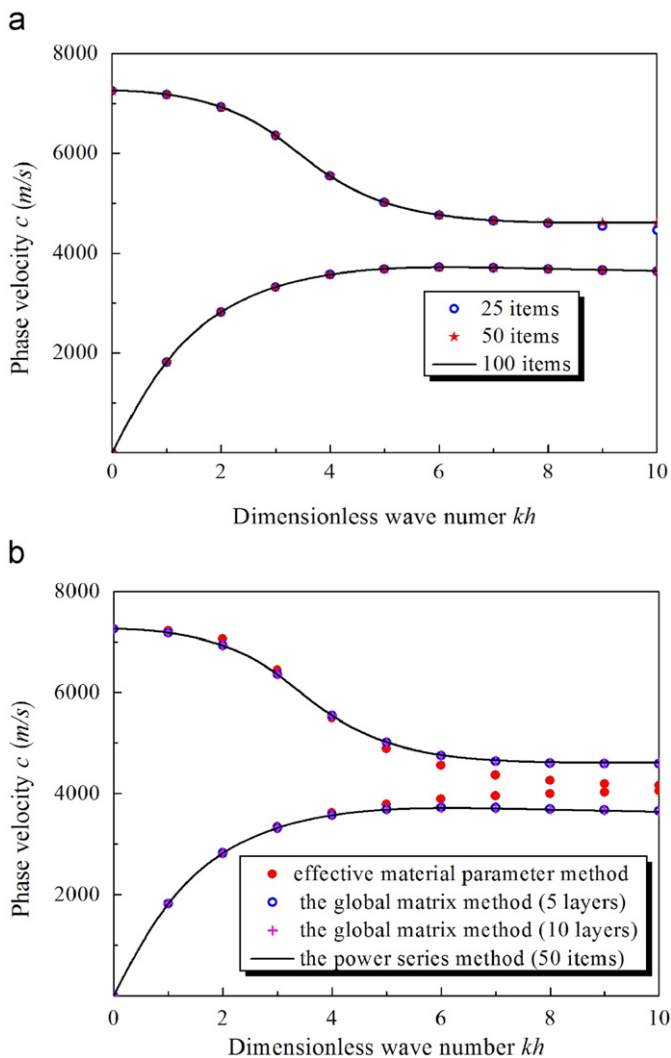


Fig. 9. Comparison of the dispersion curves solved by different methods: (a) solutions of the power series method and (b) solutions of the effective material parameter method, the power series method, and the global matrix method.

the volume fraction varies linearly, that is, $p_p = 1$ in Eq. (26). Fig. 9(a) and (b) presents the dispersion curves of the first two modes, as calculated through the present power series solution using the first

25, 50, and 100 items, the effective material method [7], and the global matrix method [3,13] with the number of the layers being either 5 or 10. For the first mode, the dispersion curves obtained by the present power series are almost identical for the cases using 25, 50, and 100 items. However, for the second mode, the dispersion curves obtained by the first 50 items coincide with those by the first 100 items, that is, for this case, the first 50 items are enough for convergence, while the error is so small that it can almost be neglected. It can be seen that the curves obtained by the global matrix method gradually approach the dispersion curves from the power series approach as the number of sub-layers increases. Considering that the order of the coefficient matrix is four times the number of layers in the global matrix method, the time complexity of the global matrix method is greater than that of the power series method. It will cost more time to use the global matrix method for 10 sub-layers than to use the power series technique for the first 50 items.

5. Conclusions

The power series method, which gives good convergence and high precision, is employed for solving the problem of Lamb waves that propagate in an FGM plate, consisting of metal and ceramics for high-temperature applications. The dispersion curves lie between those of the metallic and ceramics plates. Phase velocity depends on the gradient function and gradient coefficient. For the two kinds of FGM discussed in this paper, the whole volume fraction of metal will increase with the increase in the gradient coefficient; hence, the phase velocity will decrease and the number of modes will increase.

The influence of the gradient coefficient on the variation in the phase velocity is different in different modes. When the wavelength equals the thickness of the plate, the variation in the phase velocity in the first mode is the least, the phase velocity in the third mode is greater than that in the first mode, and the phase velocity in the second mode is clearly the greatest. Furthermore, because of the asymmetric properties of the material, the displacement components are asymmetric and the dominant positions of in-plane and out-plane displacements are different in the metal-rich and ceramic-rich surfaces.

All these results give theoretical guidance not only for experimental measurement of material properties but also for nondestructive evaluation using the ultrasonic wave generation devices.

Acknowledgement

This work was supported by the Korea Science and Engineering Foundation (KOSEF) Grant funded by the Korea government (MEST) (no. R01-2007-000-20040-0).

References

- [1] Koizumi M. The concept of FGM. Ceramic Transactions: Functionally Gradient Materials 1993;34:3–10.
- [2] Miyamoto Y, Kaysner WA, Brain BH, Kawasaki A, Ford RG. Functionally graded materials. London: Kluwer Academic Publishers; 1999.
- [3] Rose JL. Ultrasonic waves in solid media. Cambridge New York: Cambridge University Press; 1999.
- [4] Liu GR, Tani J, Ohyoshi T. Lamb waves in a functionally gradient material plates and its transient response. Part 1: Theory; Part 2: Calculation result. Transactions of the Japan Society of Mechanical Engineers 1991;57A: 131–42.
- [5] Liu GR, Han X, Lam KY. An integration technique for evaluating confluent hypergeometric functions and its application to functionally graded materials. Computers and Structures 2001;79:1039–47.

- [6] Han X, Liu GR, Lam KY, Ohyoshi T. A quadratic layer element for analyzing stress waves in FGMs and its application in material characterization. *Journal of Sound and Vibration* 2000;236:307–21.
- [7] Han X, Liu GR. Elastic waves in a functionally graded piezoelectric cylinder. *Smart Materials and Structures* 2003;12:962–71.
- [8] Qian ZH, Jin F, Wang ZK, Kishimoto K. Transverse surface waves on a piezoelectric material carrying a functionally graded layer of finite thickness. *International Journal of Engineering Science* 2007;45:455–66.
- [9] Li XY, Wang ZK, Huang SH. Love waves in functionally graded piezoelectric materials. *International Journal of Solids and Structures* 2004;41:7309–28.
- [10] Vlasie V, Rousseau M. Guide modes in a plane elastic layer with gradually continuous acoustic properties. *NDT&E International* 2004;37:633–44.
- [11] Liu J, Wang Z. Study on the propagation of Rayleigh surface waves in a graded half-space. *Chinese Journal of Applied Mechanics* 2004;21:106–9.
- [12] Cao XS, Jin F, Wang ZK. On dispersion relations of Rayleigh waves in a functionally graded piezoelectric material (FGPM) half-space. *Acta Mechanica* 2008;200:247–61.
- [13] Lowe M. Matrix techniques for modeling ultrasonic waves in multilayered media. *IEEE Transactions on Ultrasonics, Ferroelectrics and Frequency Control* 1995;42:525–42.